

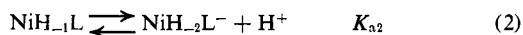
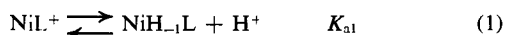
Proton Transfer Reactions of Nickel(II)-Triglycine

E. J. Billo and Dale W. Margerum¹

Contribution from the Department of Chemistry, Purdue University, Lafayette, Indiana 47097. Received January 17, 1970

Abstract: The reaction of NiH_2L^- (where L^- is the triglycinate ion and two protons are ionized from the peptide nitrogens) with H_3O^+ is 10^5 times slower than the diffusion-controlled limit. Other acids also are slow to react with NiH_2L^- and follow a general acid catalysis mechanism similar to that with CuH_2L^- . However, the rate of acid reaction with NiH_2L^- is slower than the corresponding reaction with CuH_2L^- . The addition of a second proton ($\text{NiH}_2\text{L}^- + \text{H}^+ \rightarrow \text{NiL}^+$) is very rapid in comparison to the reaction with NiH_2L^- . The kinetics of reaction of NiL^+ with base to give NiH_2L^- are first order in $[\text{NiL}^+]$ and second order in $[\text{OH}^-]$. The NiH_2L^- complex is thermodynamically unstable relative to NiH_2L^- and NiL^+ . The first and second acid ionization constants of nickel-triglycine are $10^{-8.8}$ and $10^{-7.7}$, respectively. The third acid ionization constant (to give $\text{NiH}_2\text{L}(\text{OH})^{2-}$) is $10^{-12.8}$. All rate and equilibrium constants are measured at 25.0° and an ionic strength of 0.16 M .

Ionization of peptide hydrogens from blue, octahedral nickel(II) complexes of triglycine and tetraglycine results in the formation of yellow square-planar complexes² in which the deprotonated nitrogen atoms are coordinated to nickel.³ In each complex ionization of the peptide protons occurs at approximately the same pH. Thus, Kim and Martell⁴ report that with nickel(II)-triglycine both protons are displaced in a single step in contrast to the stepwise dissociation observed with the copper complex.⁵ Although ionization of the two peptide protons from NiL^+ (where L^- is the triglycinate ion) is almost simultaneous, the acid dissociation constants K_{a1} and K_{a2} (eq 1 and 2) are measured in the present work.



Proton transfer to the deprotonated copper(II)-triglycine complex, CuH_2L^- , is much slower than normal diffusion-controlled reactions.⁶ Proton transfer reactions to NiH_2L^- are studied and found to be even slower than to CuH_2L^- .

Experimental Section

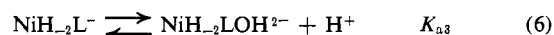
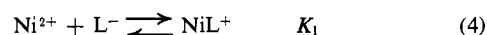
Reagents. Nickel(II) perchlorate was prepared from nickel carbonate and perchloric acid and was recrystallized from water. A nickel stock solution was prepared and was standardized by EDTA titration using murexide indicator.

Solutions of triglycine were prepared by weighing the chromatographically pure solid (Mann Research Laboratories, New York, N. Y.) and were used within a few days.

Boric acid and sodium perchlorate were recrystallized from water. Solutions of acetic acid and mono- and dihydrogen phosphate

were standardized by acid-base titration. Sodium perchlorate solutions were standardized by titration with base after passage through an ion-exchange column. All other solutions were prepared by weight from reagent grade chemicals.

Equilibrium Measurements. In addition to the equilibria in eq 1 and 2, the following equilibrium constants were determined.



The first protonation constant of triglycine, the formation constants of NiL^+ and NiL_2 , and the acid dissociation constants of NiL^+ were determined by pH titration. For the determination of the protonation constant of triglycine, a solution containing a weighed amount of triglycine (previously dried overnight *in vacuo*) was titrated with carbonate-free sodium hydroxide under an atmosphere of nitrogen. The temperature was maintained at 25.0° and the ionic strength was adjusted to 0.16 with KNO_3 . Measurements of pH were made with a Beckman research pH meter. The electrodes were calibrated with NBS buffers; pH readings were converted to $-\log [\text{H}^+]$ by subtracting 0.13 (calculated from the Davies equation⁷). The value taken for $\text{p}K_a$ was 13.75 . The formation and acid dissociation constants of the nickel complex were determined in a similar manner; four titrations were performed at different concentrations of ligand and metal.

The acid dissociation constant of NiH_2L^- , in which $\text{NiH}_2\text{L}^-(\text{OH})^{2-}$ is formed, was determined spectrophotometrically.

Kinetic Measurements. Preparation of NiH_2L^- by the addition of NaOH to solutions in which the total nickel and total ligand concentrations were equal resulted in precipitation of some nickel hydroxide. It was found that relatively stable solutions could be prepared using a ligand:metal ratio of $2:1$. No visible precipitate could be detected in these solutions for many hours, although a very small amount of precipitate became visible within 24 hr. Filtration of the solutions through a Millipore filter (Millipore Corp., Bedford, Mass.) yielded solutions from which no further precipitation occurred.

The rate of disappearance of NiH_2L^- was followed at its visible absorption maximum ($430\text{ m}\mu$, $\epsilon = 260\text{ M}^{-1}\text{ cm}^{-1}$). Rates were measured using either a Sturtevant-type stopped-flow apparatus⁸ or a Durrum-Gibson stopped-flow spectrophotometer. A Tektronix Model 564 storage oscilloscope equipped with a Polaroid

(1) Address correspondence to this author.

(2) R. B. Martin, M. Chamberlin, and J. T. Edsall, *J. Amer. Chem. Soc.*, **82**, 495 (1960).

(3) H. C. Freeman, J. M. Guss, and R. L. Sinclair, *Chem. Commun.*, 485 (1968).

(4) M. K. Kim and A. E. Martell, *J. Amer. Chem. Soc.*, **89**, 5138 (1967).

(5) M. K. Kim and A. E. Martell, *ibid.*, **88**, 914 (1966).

(6) G. K. Pagenkopf and D. W. Margerum, *ibid.*, **90**, 6963 (1968).

(7) C. W. Davies, "Ion Association," Butterworths, Washington, D. C., 1962, p 39.

(8) D. W. Margerum and J. D. Carr, *J. Amer. Chem. Soc.*, **88**, 1639 (1966).

Table I. Determination of Nickel-Triglycine Equilibrium Constants from pH Titration Data (Using $\log K_{HL} = 7.88$, at 25.0° with $\mu = 0.16 M KNO_3$)

$10^3 Ni_T,^a M$	$10^3 C_L,^a M$	Log K_1	Log K_2	Log K_{a1}	Log K_{a2}	Log $K_{a1}K_{a2}$
0.998	2.016	3.75	3.05	-8.77	-7.74	-16.51
1.996	4.032	3.70	3.10	-8.62	-7.87	-16.49
1.996	2.016	3.70	3.12	-8.83	-7.73	-16.56
2.03	6.28	3.69	3.14	-8.85	-7.71	-16.56
5.08	6.85	3.69	3.10			
	Mean values	3.71	3.10	-8.8	-7.7	-16.53
	Std dev	± 0.03	± 0.03	± 0.1	± 0.1	± 0.04

^a Initial concentration of total nickel and total triglycine.

camera was used to record the data. A few of the slowest reactions were followed with a Cary 14 recording spectrophotometer. All rates were measured at 25° . Ionic strength was adjusted to 0.16 with $NaClO_4$.

Results and Discussion

Equilibria. The formation constants of NiL^+ and NiL_2 were calculated by conventional (\bar{n}) methods, using data from the initial part of the pH titration curve (pH 5-7) where formation of deprotonated species did not interfere. Using these values, K_{a1} and K_{a2} , the acid dissociation constants of NiL^+ , were calculated from the data at higher pH (7-10) using the following equation

$$\bar{n}_H = 2 - \frac{C_L - [L^-]\{2 + K_{HL}[H^+]\} + [Ni^{2+}]\{2 + 2\beta_2[L^-]^2\} - S}{C_L - [L^-]\{1 + K_{HL}[H^+]\} - 2\beta_2[Ni^{2+}][L^-]^2} \quad (7)$$

where $\beta_2 = K_1K_2$ and C_L is the concentration of all forms of triglycine

$$S = [ClO_4^-] + [OH^-] - [Na^+] - [H^+] \quad (8)$$

$$[Ni^{2+}] = \frac{C_L + \gamma S + [L^-]\{\gamma - 1 - K_{HL}[H^+]\}}{2\gamma + (1 + \gamma)\beta_1[L^-] + 2\beta_2[L^-]^2} \quad (9)$$

$[L^-]$ is the positive root of

$$\beta_2[Ni^{2+}][L^-]^2 + \{K_{HL}[H^+] + 1\}[L^-] + \{C_M - C_L - [Ni^{2+}]\} = 0 \quad (10)$$

and

$$\gamma = 1 + [H^+]/K_{a2} \quad (11)$$

The method of solution involved a double iteration. Initially, K_{a2} was set equal to 1 in eq 11, and for each experimental point on the titration curve, $[Ni^{2+}]$ and $[L^-]$ were obtained by iteration between eq 9 and 10. Iteration was terminated when the change in free ligand concentration between successive cycles was less than 0.01%. The value of \bar{n}_H , the average number of protons bound to NiH_2L^- , was then calculated using eq 7. When \bar{n}_H had been calculated for all experimental

points, K_{a1} and K_{a2} were obtained from the slope and intercept of the least-squares fit of⁹

$$\frac{\bar{n}_H}{(\bar{n}_H - 1)[H^+]} = \frac{(2 - \bar{n}_H)[H^+]K_{a1}K_{a2}}{(\bar{n}_H - 1)} - K_{a2} \quad (12)$$

About 16 values of \bar{n} were taken between 0.2 and 0.8 and between 1.2 and 1.8 for the calculation. The new value of K_{a2} was substituted into eq 11 and the process repeated until the change in K_{a2} between successive cycles was less than 0.1%. The constants obtained for four titrations are given in Table I.

From pH 10 to 11.5, the titration curve indicated that no further deprotonation of NiH_2L^- occurred, although Kim and Martell⁴ reported $\log K_{a3} = -10.5$. However, above pH 12 the yellow solution of NiH_2L^- became orange and conversion to a new species appeared to be complete in concentrated base ($\sim 5 M NaOH$), $\lambda_{max} 475 m\mu$, $\epsilon 167 M^{-1} cm^{-1}$. Neutralization of the excess base restored the original spectrum of NiH_2L^- . Neither the spectra (which included an isobestic point) nor the equilibrium constant was affected when the ligand:metal ratio was decreased from 2:1 to 1:1. Thus, the orange species is presumably NiH_2LOH^{2-} . Spectrophotometric measurements were used to determine K_{a3} because the pH required to obtain complete formation of NiH_2LOH^{2-} was extremely high. The nickel concentration was $4.9 \times 10^{-4} M$, the triglycine concentration was twice as great, and five measurements at $430 m\mu$ (5-cm cell) were taken from pH 12-13. The dissociation constant ($K_{a3} = 10^{-12.8}$) and the extinction coefficient (ϵ , at $430 m\mu$, $127 M^{-1} cm^{-1}$) of NiH_2LOH^{2-} were obtained by a graphical method.

A summary of the equilibrium constants reported by earlier workers and those from the present work is given in Table II. With the exception of Piehl's¹⁰ value for K_1 , the values of K_{HL} , K_1 , and K_2 obtained in the present work and in previous studies are in excellent agreement, when differences in ionic strength are considered. The previous determination² of K_{a1} and K_{a2} was an approximation, which, as the authors pointed out, needed an iterative calculation to be more accurate. This has been done by a more precise method in the

(9) F. J. C. Rossotti and H. Rossotti, "The Determination of Stability Constants," McGraw-Hill, New York, N. Y., 1961, p 92.

(10) D. H. Piehl, Ph.D. Thesis, University of Iowa, Iowa City, Iowa, 1966.

Table II. Nickel-Triglycine Equilibrium Constants (25.0°)

Ref	μ^a	Log K_{HL}	Log K_1	Log K_2	Log K_3	Log K_{a1}	Log K_{a2}	Log $K_{a1}K_{a2}$	Log K_{a3}
2	0.16 (KNO ₃)	8.01	3.70	2.90	2	-8.25	-8.45	-16.70	
4	0.10 (KNO ₃)	7.90	3.76	3.10				-16.9	-10.5
10	0.10 (KNO ₃)	7.97	2.84			-8.9	-8.1	-17.0	
This work	0.16 (KNO ₃)	7.88 ^b	3.71 ^c	3.10 ^c		-8.8 ^d	-7.7 ^d	-16.53 ^e	-12.8 ^d

^a Ionic strength. ^b ± 0.01 . ^c ± 0.03 . ^d ± 0.1 . ^e ± 0.04 .

present work. Kim and Martell⁴ were nearly correct in assigning a simultaneous ionization of two protons. Although the maximum concentration of the intermediate species $NiH_{-1}L$ never exceeded 5% of the total nickel concentration during the titrations, we were able to calculate its ionization constant with reasonable accuracy. As indicated in Table II the product $K_{a1}K_{a2}$ is known to better precision than the individual constants.

There is a major difference between the value of log K_{a3} determined by Kim and Martell (-10.5) and in the present work (-12.8). The former value is unusually low for hydrolysis of a nickel chelate, especially since coordination of hydroxide may involve displacement of the peptide carboxylate group in order to maintain a square-planar complex. Similar values of log K_a were found by Kim and Martell^{2,3} for the hydrolysis of $CuH_{-2}L^-$ (log $K_{a3} = -10.9$) and for the analogous nickel complex of tetraglycine, $NiH_{-3}L^{2-}$ (log $K_{a4} = -10.0$). Other workers, however, have found much higher values for these hydrolysis constants: $CuH_{-2}L^-$, log $K_{a3} = -11.9$,¹¹ -12.0;¹² for tetraglycine, $NiH_{-3}L^{2-}$, no addition of OH^- was detectable even in 1 M sodium hydroxide.¹²

The unusual nature of the acid dissociation equilibria involving NiL^+ , $NiH_{-1}L$, and $NiH_{-2}L^-$ is evident from the values of log K_{a1} and log K_{a2} . The formation of $NiH_{-2}L^-$ from $NiH_{-1}L$ occurs more readily than does the formation of $NiH_{-1}L$ from NiL^+ . This is the result of a change in the electronic state and coordination from octahedral ($NiH_{-1}L$) to square planar ($NiH_{-2}L^-$). Many equilibria involving a change in metal-atom ground state from high spin to low spin exhibit similar increases in stability of the low-spin complex, e.g., the iron(II) complexes of 1,10-phenanthroline, and $Ni(CN)_4^{2-}$.

Kinetics. The rate of disappearance of $NiH_{-2}L^-$ was studied from pH 4 to 13. The concentrations of $NiH_{-2}L^-$ (0.5 - 2.0×10^{-3} M) and of buffer (0.5 - 2.0×10^{-2} M) were such that the reaction was pseudo first order in $NiH_{-2}L^-$. For each of the weak acids studied, the pH profile was determined in the pH range of the buffer and at two to five different buffer concentrations. At pH 5, the rate was unaffected by moderate changes in the concentration of excess triglycine or by the addition of low concentrations ($\sim 10^6$ M) of copper(II). The rate constants observed for acetic acid, hydrogen maleate, and dihydrogen phosphate buffer systems are listed in Table III ($[HX]_T$ is the total concentration of buffer acid and its conjugate base).

(11) W. L. Koltun, R. H. Roth, and F. R. N. Gurd, *J. Biol. Chem.*, **238**, 124 (1963).

(12) E. J. Billo, unpublished observations.

Table III. Reaction of $NiH_{-2}L^-$ with Weak Acids (25°, 0.16 M NaClO₄)

HX = acetic acid			HX = Hmaleate ⁻		
$[HX]_T$, M	-Log $[H^+]$	k_{obsd} , sec ⁻¹	$[HX]_T$, M	-Log $[H^+]$	k_{obsd} , sec ⁻¹
0.030	4.16	22.1	0.015	5.29	1.76
0.030	4.45	14.8	0.015	5.62	1.24
0.030	4.76	10.2	0.015	5.87	0.87
0.030	5.27	3.86	0.015	6.47	0.32
0.050	4.06	60	0.025	5.02	3.06
0.050	4.17	45	0.025	5.40	2.10
0.050	4.45	31	0.025	5.74	1.45
0.050	4.55	26.5	0.025	6.08	0.92
0.050	4.55	27.6	0.025	6.19	0.77
0.050	4.66	24	0.025	7.35	0.18
0.050	4.70	21.5	0.040	4.79	5.33
0.050	4.79	12.7	0.040	4.97	4.27
0.050	4.99	19.8	0.040	5.27	3.54
0.050	5.10	12.0	0.040	5.56	2.81
0.050	5.39	5.2	0.040	5.75	2.25
0.050	5.44	5.0	0.050	5.28	4.20
0.050	6.15	2.1	0.050	5.48	3.61
0.100	4.15	74	0.060	4.87	7.3
0.100	4.38	68	0.060	4.89	6.8
0.100	4.37	68	0.060	5.19	5.24
0.100	4.46	63	HX = H ₂ PO ₄ ⁻		
0.100	4.58	50	0.0125	6.08	6.0
0.100	4.67	45	0.0125	6.50	4.35
0.100	4.71	38.5	0.0125	6.90	2.88
0.100	5.04	19.4	0.0125	7.22	1.44
0.100	5.36	11.1	0.0250	5.83	12.7
0.100	5.69	5.20	0.0250	6.14	10.6
0.100	6.22	2.10	0.0250	6.64	7.3
			0.0250	7.29	2.56
			0.0250	7.73	1.19

By using appropriate acid-base indicators in similar experiments in which the buffer was not in large excess, it was possible to show that protons were not added to $NiH_{-2}L^-$ in a rapid reaction before the observed rate, as had been suggested.¹³ Thus, there is not a thermodynamically stable species $Ni(H_{-2}L)H$ observable above pH 4. This does not preclude such a species as a kinetically important reaction intermediate however. Higher acidities could not be used because the rate of disappearance of the square-planar complex itself becomes too rapid to detect any protonated intermediates.

The reaction of $NiH_{-2}L^-$ with excess HX (acetic acid, hydrogen maleate, or dihydrogen phosphate) followed the rate expression

$$\frac{-d[NiH_{-2}L^-]}{dt} = k_{obsd}[NiH_{-2}L^-] \quad (12a)$$

(13) P. I. Chamberlain, Ph.D. Thesis, State University of New York at Buffalo, Buffalo, N. Y., 1968.

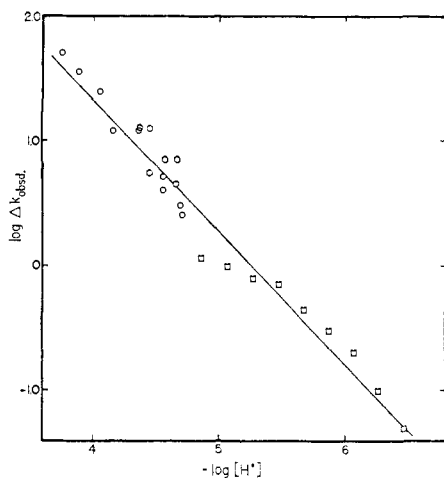


Figure 1. Plot of data used to determine $k_{H_3O^+}$. For reactions with HX = acetic acid (O), $\Delta k_{\text{obsd}} = k_{\text{obsd}} - k_{\text{HX}}[\text{HX}]$; for reactions with HX = hydrogen maleate (\square), Δk_{obsd} was obtained by extrapolation to zero of k_{obsd} values obtained at several concentrations of Hmaleate $^-$. The straight line is the least-squares line and has a slope of 1.06 ± 0.06 .

where

$$k_{\text{obsd}} = k_{\text{HX}}[\text{HX}] + k_{\text{H}}[\text{H}_3\text{O}^+] \quad (12b)$$

A plot of the logarithm of the buffer-independent part of the observed rate ($k_{\text{H}}[\text{H}_3\text{O}^+]$) vs. $-\log [\text{H}^+]$ (Figure 1) was linear from pH 4 to 6 with a slope of 1.06 ± 0.06 , demonstrating that the reaction was first order in H_3O^+ . The k_{HX} and k_{H} values are listed in Table IV.

Table IV. Rate Constants for Proton Transfer to NiH_2L^- (25°, 0.16 M NaClO $_4$)

HX	$\text{p}K_{\text{a}}$	$k_{\text{HX}}, M^{-1} \text{sec}^{-1}$
H_3O^+	-1.74	$(2.0 \pm 0.8) \times 10^6$
HOAc	4.49	$(9.7 \pm 0.3) \times 10^2$
Hmaleate $^-$	5.70	$(1.0 \pm 0.1) \times 10^2$
H_2PO_4^-	6.69	$(4.8 \pm 0.2) \times 10^2$
H_3BO_3	9.00	Less than 10^{-1}
H_2O	15.49	9.0×10^{-4}

The reaction also was studied in the pH range 8–9, using boric acid–sodium borate buffers. In this pH range the reaction is reversible and the hydrogen ion concentration is buffered. As a result, the reaction observed is given in eq 13 and the observed first-order



rate constant is the sum of k_a and k_b . The value of k_{obsd} increases with increasing pH as shown in Figure 2. A plot of k_{obsd} against $[\text{OH}^-]^2$ gave a linear plot which is in accord with the mechanism given in eq 14 and 15,

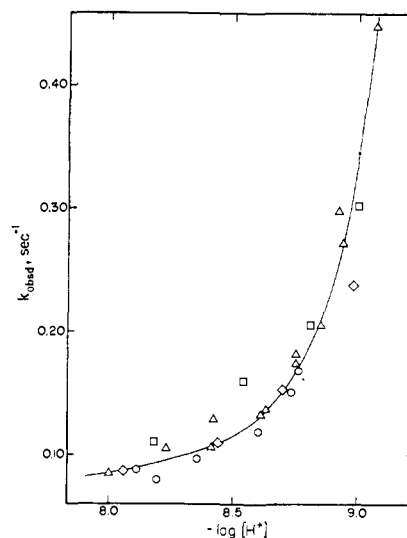
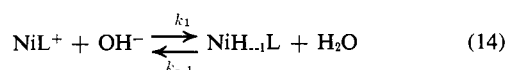
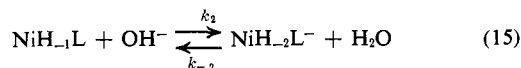


Figure 2. Observed first-order rate constants for the reversible equilibration of NiH_2L^- and NiL^+ in boric acid, sodium borate buffer, $\mu = 0.16 M$ (NaClO $_4$), 25.0°; total buffer concentration, 0.02 (O), 0.05 Δ , 0.08 (\square), and 0.12 M (\diamond).



because the concentration of NiH_2L^- can be neglected. This gives

$$k_{\text{obsd}} = k_{-2} + \frac{k_1 k_2}{k_{-1}} [\text{OH}^-]^2 \quad (16)$$

and the plot of eq 16 gives $k_{-2} = 0.088 \pm 0.004 \text{ sec}^{-1}$ and $k_1 k_2 / k_{-1} = (2.5 \pm 0.1) \times 10^9 M^{-2} \text{ sec}^{-1}$. The ratio of rate constants, $k_1 k_2 / k_{-1} k_{-2}$, times K_w^2 equals 10^{-17} , in fair agreement with the potentiometric value for $K_{a1} K_{a2}$.

The protonation of NiH_2L^- also was studied using boric acid–sodium borate buffers, with EDTA added to act as a scavenger. (As was observed⁶ with CuH_2L^- , monoprotonated EDTA does not react directly with NiH_2L^- .) Under these conditions, reversibility is prevented and $k_{\text{obsd}} = k_{-2}$. Over the pH range 8–10, and with $[\text{EDTA}]_{\text{T}} = (2.1\text{--}10.7) \times 10^{-3} M$, $k_{-2} = 0.088 \pm 0.010 \text{ sec}^{-1}$. Boric acid (0.02–0.12 M) had no effect on k_{obsd} . Hence the k_{HX} value for H_3BO_3 must be less than $10^{-1} M^{-1} \text{ sec}^{-1}$.

In both the reversible and the EDTA reactions there was excess triglycine present in solution. Although the presence of triglycine did not affect the reactions at pH 5, there is a small effect on the rates at higher pH. A study of k_{-2} as a function of excess triglycine indicated that this rate constant was slightly increased by excess triglycine at pH 9, and extrapolation to zero excess triglycine yielded $k_{-2} \cong 0.05 \text{ sec}^{-1}$. This value for the reaction of H_2O with NiH_2L^- was divided by 55.5 to give the second-order rate constant of $9 \times 10^{-4} M^{-1} \text{ sec}^{-1}$ given in Table IV.

Above pH 10, k_{obsd} for the reaction of NiH_2L^- and EDTA was no longer independent of EDTA. The observed rate was first order in NiH_2L^- concentration and the observed first-order rate constant with excess

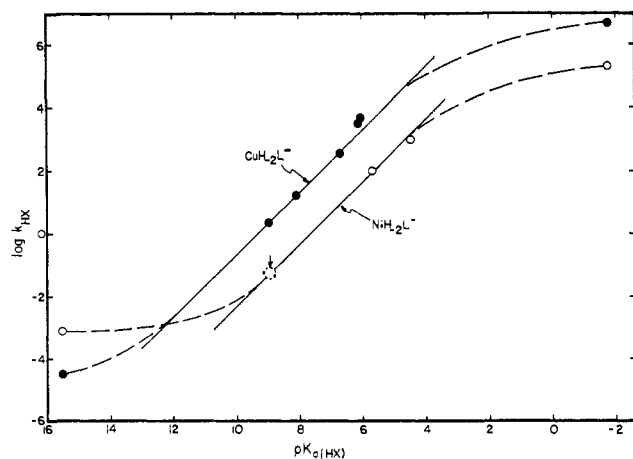


Figure 3. Rate constants for the reaction of MH_2L^- with HX as a function of the acidity of HX. The solid lines correspond to a Brønsted α value of unity. The arrow indicates that the k_{HX} value for the H_3BO_3 reaction with NiH_2L^- is below this value; the value is believed to fall within the dashed circle.

EDTA had an EDTA-independent component (k') and an EDTA-dependent component (k'')

$$k_{\text{obsd}} = k' + k''[\text{EDTA}]_T$$

(Below pH 10, $k'' \approx 0$ and $k' = k_{-2}$.) Both k' and k'' were pH dependent; k' decreased with increasing pH and was essentially zero at pH 12, while k'' increased with increasing pH. Like k_{-2} , the rate step represented by k'' appeared to be catalyzed by triglycinate.

The decrease in k_{-2} above pH 10 (in reactions in which EDTA provided the driving force) is probably the result of hydroxide competing with EDTA, by reacting with $NiH_{-1}L$, to force the reaction back toward $NiH_{-2}L^-$. This mechanism qualitatively explains the observed behavior, but because of triglycinate catalysis of both the EDTA-dependent and EDTA-independent reactions, the system was not studied further. Triglycinate catalysis of the reaction between $CuH_{-2}L^-$ and EDTA has also been observed and the reaction sequence is not a simple one. In the present work leading to the mechanisms in Figure 4 the triglycinate catalysis was either negligible or the data were corrected for it.

Finally, the rate of disappearance of $NiH_{-2}L^-$ was inhibited by moderate concentrations of 2,6-lutidine buffer. The mechanism of this inhibition will be the subject of a future communication.

Discussion of the Observed Kinetics. The rate law observed for the reactions of acids with $NiH_{-2}L^-$ is consistent with eq 17 (letting HX include H_3O^+ and H_2O). The $NiH_{-1}L$ complex which is formed reacts rapidly with HX to give NiL^+ (or $Ni^{2+} + HL$). The faster transfer of the second proton (eq 18) can be under-



stood in terms of the difference in the electronic state and coordination of the two complexes. The diamagnetic, square-planar $NiH_{-2}L^-$ complex would be ex-

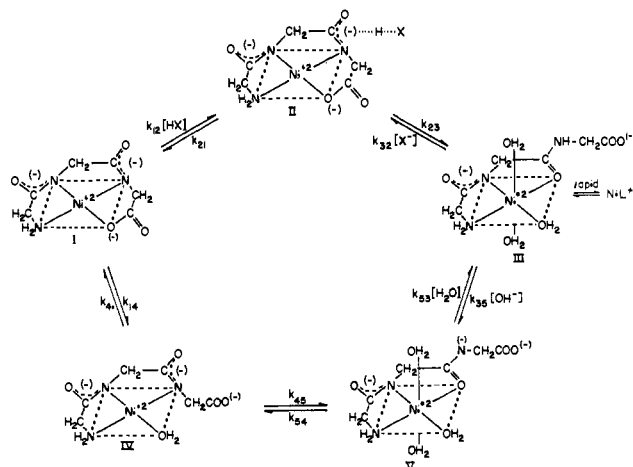


Figure 4. One proposed mechanism for the reaction of $NiH_{-2}L^-$ (I) with acid (HX) and with water to form $NiH_{-1}L$ (III). Mechanism A corresponds to the I-II-III path with the rate-determining step between II and III. Mechanism B is not shown in this diagram, but one preequilibrium step could correspond to the formation of IV which then reacts with acids in a rate-determining process. The I-IV-V-III pathway corresponds to the acid-independent dissociation where the rate-determining step is between IV and V.

pected to have much stronger coordination of the peptide nitrogen than the paramagnetic, octahedral $NiH_{-1}L$ complex. As a result it is more difficult to transfer a proton to the peptide nitrogen and to break the nickel-peptide bond in $NiH_{-2}L^-$.

The kinetics of the addition of the first proton to $NiH_{-2}L^-$ is similar to that found⁶ for the reaction of $CuH_{-2}L^-$. Figure 3 shows the parallel dependence of the copper and nickel complexes in plots of $\log k_{HX}$ against the pK_a value of HX. With both metals the slope of the plot, which corresponds to the Brønsted α value,¹⁴ is unity for acids with pK_a values from 9 to 5. The reaction of nickel-triglycinate with H_3O^+ has a rate constant of $2 \times 10^5 M^{-1} \text{sec}^{-1}$ which is 25 times slower than the reaction of copper-triglycinate with H_3O^+ . In the region where $\alpha = 1$, the k_{HX} values (for a given pK_a of HX) are about 50 times slower with $NiH_{-2}L^-$ than with $CuH_{-2}L^-$. The behavior of the nickel systems in the $\alpha = 1$ region is based on the rate constants obtained for acetic acid, hydrogen maleate, and the limiting value for boric acid. As mentioned earlier, general acid catalysis by boric acid has a k_{HX} value less than $0.1 M^{-1} \text{sec}^{-1}$. The $\alpha = 1$ slope predicts a value of $0.04 M^{-1} \text{sec}^{-1}$ for H_3BO_3 , but this is difficult to establish because of the first-order reaction of the solvent with $NiH_{-2}L^-$ ($k_{-2} = 0.088$ in eq 15).

The rate constant for the reaction of $H_2PO_4^-$ with $NiH_{-2}L^-$ is anomalously large and it is omitted from Figure 3. The predicted value, corresponding to the acid strength of $H_2PO_4^-$, is $10 M^{-1} \text{sec}^{-1}$, while the observed rate constant is $480 M^{-1} \text{sec}^{-1}$.

It is known¹⁵ that coordinating ligands can speed the first steps in the loss of triglycinate for $NiH_{-2}L^-$. The $H_2PO_4^-$ ion could act in this manner as a nucleophile or could act as both a coordinating ligand and an acid.

(14) R. P. Bell, "The Proton in Chemistry," Methuen and Co. Ltd., London, 1959, p 155.

(15) E. J. Billo, D. W. Margerum, and G. F. Smith, manuscript in preparation.

A similar, but smaller acceleration was noted⁶ in the reaction of $H_2(EDTA)^{2-}$ and $H_2(CyDTA)^{2-}$ with $CuH_{-2}L^-$, and these points fall above the $\alpha = 1$ slope in Figure 3.

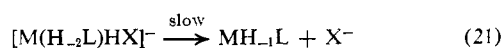
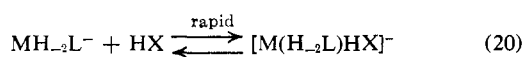
The acid-independent dissociation rate constant for $NiH_{-2}L^-$ (k_{-2}) makes a larger contribution relative to the k_{HX} rate constants than is the case for $CuH_{-2}L^-$. As a result, it was difficult to compare the reactions of the same acids with both complexes. It was this effect which made the kinetic contribution of 0.1 M H_3BO_3 negligible with $NiH_{-2}L^-$. The difficulty was compounded by the inhibition caused by 2,6-lutidine and the need to avoid acids which could act as strong coordinating agents as well as proton donors (such as $H_2PO_4^-$ and H_2EDTA^{2-}). Another limiting factor is encountered in attempting to use acids of pK_a less than 4. That factor is the stopped-flow mixing system in which reaction half-lives need to be greater than about 5 msec. The data in Table III show that this limit was approached using 0.1 M acetic acid at pH 4.1 where half-lives of 10 msec were measured.

In Figure 3 the shift of the k_{HX} values for $NiH_{-2}L^-$ compared to $CuH_{-2}L^-$ does not correspond to the relative basicity of the two complexes for the reaction in eq 19. In fact, quite the opposite behavior would be



expected from this reaction in which $NiH_{-2}L^-$ is a stronger base than $CuH_{-2}L^-$ by a factor of 12 ($pK_{a2} = 7.7$ for $NiH_{-1}L$ and 6.6 for $CuH_{-1}L$). The protonation reactions are not as simple as eq 19 implies, but involve substantial changes in the groups which are coordinated to the metal ion. The $MH_{-2}L^-$ complex loses a peptide nitrogen-metal bond and a carboxylate-metal bond in forming $MH_{-1}L$, which for corresponding solids¹⁶ has a peptide oxygen-metal bond. Although the slower reaction of the $NiH_{-2}L^-$ complex compared to the $CuH_{-2}L^-$ complex does not correspond to their relative basicities, it does agree with the generally slower coordination substitution reactions of nickel compared to copper. More specifically, it also agrees with the relative rates of nucleophilic displacement of triglycine from nickel and copper by ammonia and polyamines.^{15,17}

Proposed Reaction Mechanisms. Mechanism A for the reaction of $NiH_{-2}L^-$ with acids is similar to that already proposed for $CuH_{-2}L^-$ in which the rate-determining step is a metal-N(peptide) bond cleavage after interaction of the acid. In the reaction sequence in eq 20 and 21 the $[M(H_{-2}L)HX]^-$ species is not present in



appreciable concentrations and must rearrange to give $MH_{-1}L^-$.

(16) J. D. Bell, H. C. Freeman, A. M. Wood, R. Driver, and W. R. Walker, *Chem. Commun.*, 1441 (1969).

(17) G. K. Pagenkopf and D. W. Margerum, *J. Amer. Chem. Soc.*, 92, 2683 (1970).

Direct experimental evidence exists for protonated intermediates which retain metal-N(peptide) bonds in Co(III) complexes. Thus, the bis(glycylglycinato)cobaltate(III) anion in eq 22 adds two protons at low pH



to give the bis(glycylglycinato)cobalt(III) cation.¹⁸ Recent crystal structures¹⁹ show that the proton adds to the O(peptide) rather than to the N(peptide). The proton addition increases the double bond character of the C-N bond and decreases that of the C-O bond. The proton addition also lengthens the Co-N(peptide) bond from 1.87 to 1.94 Å. The pK_a of the protonated cobalt(III) complex was first reported²⁰ to be about 1.2, but recent²¹ nmr data suggest a pK_a value of 0.5. The proton addition is rapid and the nmr data show that the half-life is less than $1/30$ sec at pH 0.5, 35°. The protonated bis(glycylglycinato)cobalt(III) complex is slow to break the Co-N(peptide) bond, but its dissociation is much faster than in more dilute acid.²¹ Therefore, this Co(III) complex provides evidence of a reaction mechanism in agreement with eq 20 and 21.

A more detailed representation of mechanism A is given in Figure 4 in the I-II-III reaction path. The intermediate II corresponds to $[M(H_{-2}L)HX]^-$ and is drawn to indicate the possibility that the proton may go to either the O(peptide) or the N(peptide) in the kinetic intermediate. Although the O(peptide) is the more basic site and is protonated in the Co(III) complexes, it is nevertheless possible that protonation of the N(peptide) is more important kinetically because this would lead to a much weaker metal-N(peptide) bond. The terminal carboxylate group is shown as bonded to the metal during the initial proton transfer. However, this group must break its coordination in order to go from I to III and this may occur before the proton transfer step rather than afterwards.

In order to have general acid catalysis (as opposed to only H_3O^+ catalysis) the intermediate $[M(H_{-2}L)HX]^-$ must have X^- associated with it. If there were complete transfer of the proton from HX to give $[M(H_{-2}L)H]$ in the preequilibrium step there would be only H_3O^+ catalysis. The acid strength of $M(H_{-2}L)H$ is much greater than any other acid except H_3O^+ . At the same time the HX acids are better proton donors than water, and a reaction intermediate with hydrogen bonding to HX is not unreasonable. The fact that $\alpha = 1$ for various HX acids is consistent with the proposed mechanism in which the extent to which the proton is transferred from X in $[Ni(H_{-2}L)HX]^-$ is in direct proportion to the acidity of HX. This would be true whether HX were associated with the O(peptide) or the N(peptide).

One difficulty with mechanism A is that it does not directly account for the fact that in Figure 3 the rate constants for the H_3O^+ reactions with $CuH_{-2}L^-$ and $NiH_{-2}L^-$ tend to level off well below the diffusion-controlled values and are smaller than predicted from

(18) R. D. Gillard, P. M. Harrison, and E. D. McKenzie, *J. Chem. Soc. A*, 618 (1967).

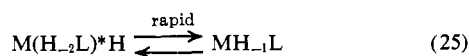
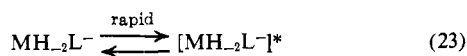
(19) M. T. Barnet, H. C. Freeman, D. A. Buckingham, I. Hsu, and D. van der Helm, *Chem. Commun.*, 367 (1970).

(20) R. D. Gillard and M. G. Price, *J. Chem. Soc. A*, 1813 (1969).

(21) R. D. Gillard and P. R. Mitchell, personal communication.

the $\alpha = 1$ slope for other acids. Other reasons have to be postulated for the special behavior of H_3O^+ .

Mechanism B suggests that the MH_{-2}L^- complex has to undergo a rapid but unfavorable equilibration (eq 23) before it can react with HX and that the speed of the HX reaction (eq 24) is the rate-determining step.

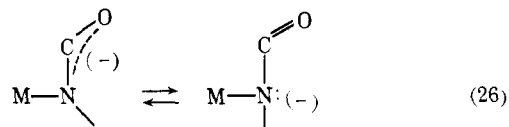


This mechanism will account for the shape of the curve in Figure 3 if the $\text{p}K_a$ of $\text{M}(\text{H}_{-2}\text{L})^*\text{H}$ is about 2. With H_3O^+ the reaction in eq 24 will be limited by the diffusion-controlled rate ($\sim 10^{10} \text{ M}^{-1} \text{ sec}^{-1}$), which means the preequilibration step in eq 23 must be about 10^{-5} for $\text{NiH}_{-2}\text{L}^-$ and about 10^{-3} for $\text{CuH}_{-2}\text{L}^-$. A region of $\alpha = 1$ will be expected for k_{HX} when the $\Delta\text{p}K$ (the $\text{p}K_a$ of $\text{M}(\text{H}_{-2}\text{L})^*\text{H}$ less the $\text{p}K_a$ of HX) values become less than -2 .²² Thus, because $\text{M}(\text{H}_{-2}\text{L})^*\text{H}$ is a moderately strong acid, the rate of its formation from the weaker acid HX will depend directly on the acidity of HX .

The rearrangement indicated in eq 23 cannot involve the complete dissociation of the metal–N(peptide) bond because this would give an extremely strong base which would show no discrimination in its reaction with various acids. The $\text{p}K_a$ value needed for the $\text{M}(\text{H}_{-2}\text{L})^*\text{H}$ intermediate is of the same order of magnitude as that found for the O(peptide) protonation in the bis(glycylglycinato)cobalt(III) complex. A possible structure for $[\text{MH}_{-2}\text{L}^-]^*$ is the triglycine complex with a free carboxylate group as in structure IV (Figure 4). It might react with acids by protonation of the peptide group in accord with eq 24. The subsequent shift of coordinate groups in eq 25 need only have a half-life less than 1 msec (or a first-order rate constant greater than about 10^3 sec^{-1}) to go undetected in the stopped-flow experiments.

Although mechanism B provides an explanation of the $\log k_{\text{HX}}$ vs. $\text{p}K_{a(\text{HX})}$ plots for each metal complex there are again some difficulties. First of all this mechanism cannot apply to Co(III), where protonation is known to occur before the slow metal–peptide bond rupture. Secondly, the copper–triglycine complex is more stable than the nickel–triglycine complex, yet the preequilibration step in eq 23 has to be less favorable for nickel than for copper. Thirdly, a terminal nickel–peptide linkage in the nickel–tetraglycine complex ($\text{NiH}_{-3}\text{L}'^{2-}$) appears to react with H_3O^+ at about the same rate as the triglycine complex,²³ but in the tetraglycine case a preequilibrium of the terminal carboxylate chelate cannot be involved.

A different type of preequilibration step can be postulated for eq 23. As the trigonal nitrogen in the peptide becomes more tetrahedral (eq 26) and accepts the nega-



tive charge it becomes a better site for the proton-transfer reaction. This type of electronic and structural rearrangement has been postulated in the reaction of some carbon acids whose conjugate bases react at less than diffusion-controlled rates with H_3O^+ . Normally, acids would be expected to assist the electronic rearrangement, and often gradual changes in α values are found when protonation is accompanied by marked alteration of steric structure.²² This is in contrast to the fairly sharp transition of the α value between H_3O^+ and the other acids in Figure 3. However, in the present case we have seen that normally the O(peptide) is the more basic site and a step to concentrate the charge on the N(peptide) may not be assisted by a nearby HX molecule. If a proton is transferred to the N(peptide), the coordinate bond to the metal would become very weak and easily broken.

Each of the mechanisms mentioned has some favorable and unfavorable aspects, and at present it is not possible to conclude which one is more likely.

Mechanism of Acid-Independent Dissociation. The reversible kinetic studies at pH 8–9 and the EDTA displacement reactions at pH 8–10 necessitate another reaction path. In both studies the acid-independent dissociation rate constant (k_{-2}) is many orders of magnitude larger than possible if H_2O acted only as an acid. The mechanism I–IV–V–III in Figure 4 is proposed, where the ligand first breaks the carboxylate bond and then the peptide bond in the rate-determining step (k_{45}). Once the deprotonated peptide–nitrogen group is free of the nickel it is a very strong base and the proton transfer from H_2O is fast. The I–IV–V–III mechanism may be considered as a solvent dissociation path which accompanies the acid dissociation path (either mechanism A or B).

A value for $k_2 = 2.8 \times 10^4 \text{ M}^{-1} \text{ sec}^{-1}$ can be calculated from $k_1 k_2 / k_{-1} = 2.5 \times 10^9 \text{ M}^{-2} \text{ sec}^{-1}$ and from $\log(k_1 / k_{-1}) = 13.75 - 8.8$. The k_2 value is in agreement within a factor of 2 with that calculated from $k_{-2} = 0.05 \text{ sec}^{-1}$ and $\log(k_2 / k_{-2}) = 13.75 - 7.7$. This rate constant for the reaction of NiH_{-1}L and OH^- is several orders of magnitude greater than would be expected from the reverse steps III–II–I and also requires the alternate reaction path III–V–IV–I. In this mechanism k_2 corresponds to $(k_{35} / k_{33}) k_{51}$. A similar mechanism was needed in the reaction of CuH_{-1}L and OH^- .

The acid-independent dissociation rate constant for $\text{NiH}_{-2}\text{L}^-$ (corresponding to $k_{14} k_{45} / k_{41}$ in Figure 4) is 0.05 sec^{-1} when treated as a first-order process corrected for triglycine catalysis. This compares to a value of $1.8 \times 10^{-3} \text{ sec}^{-1}$ calculated⁶ for the corresponding reaction of $\text{CuH}_{-2}\text{L}^-$. Thus, the acid attack on MH_{-2}L^- is 25–50 times faster for copper than for nickel, but the solvent attack is only $1/30$ th as fast for the copper complex as it is for the nickel complex.

There are many similarities in the kinetic behavior of the $\text{NiH}_{-2}\text{L}^-$ and $\text{CuH}_{-2}\text{L}^-$ complexes and for both metals rearrangement of the triglycine coordination appears to contribute to their much slower than diffu-

(22) M. Eigen, *Angew. Chem., Int. Ed. Engl.*, **3**, 1 (1964).

(23) E. B. Paniago, D. W. Margerum, and D. C. Weatherburn, unpublished work.

sion-controlled reactions with H_3O^+ . Additional work is needed before a decision can be made concerning alternate mechanisms A and B. The thermodynamic and kinetic behavior of the nickel–triglycine complexes also differ from those of the copper–triglycine complexes because of the relative instability of $NiH_{-1}L$.

Acknowledgment. Helpful discussions with Professors M. Eigen and F. A. Long are gratefully acknowledged. This investigation was supported by National Science Foundation Grant No. GP6725X, and by Public Health Service Research Grant No. GM-12152 from the National Institute of General Medical Sciences.

Chelation of Uranyl Ions by Adenine Nucleotides. IV. Nuclear Magnetic Resonance Investigations, Hydrogen-1 and Phosphorus-31, of the Uranyl–Adenosine 5′-Diphosphate and Uranyl–Adenosine 5′-Triphosphate Systems¹

Kenneth E. Rich, Raghunath T. Agarwal,² and Isaac Feldman³

Contribution from the Department of Radiation Biology and Biophysics, University of Rochester School of Medicine and Dentistry, Rochester, New York 14620. Received April 4, 1970

Abstract: Nmr spectra, 1H (100 MHz) and ^{31}P (40 MHz), were obtained for uranyl nitrate–adenosine diphosphate (U–ADP) and –adenosine triphosphate (U–ATP) mixtures in D_2O having various stoichiometries and basicities over the pD range ≈ 7 –11. The spectra show that from pD 7.7 to 11 an equimolar U–ATP mixture consists of 2:2 sandwich-type (ST) dimeric chelates, **2**, in which the ligands are the β and γ phosphoryl groups and the ribose hydroxyls, but from pD 6.8 to 7.3 non-ST chelates, in which the uranium is bound only to the β and γ phosphoryl groups, predominate. About 10% of the complex is in the ST form at pD 7.3 in 1:1, 0.05 *M* U–ATP solution, but none is present in a 1:2 solution with the same pD and uranium concentration. Unlike the U–ATP and U–AMP systems, the U–ADP system does not contain 2:2 ST complexes at any pD. Rather, at pD 7.7 only non-ST complexes (**4** and **5**), in which uranium is chelated by the two phosphoryl groups, exist in 1:1 and 1:2 U–ADP mixtures, but these disproportionate to 4:2 ST chelates and free ADP above pD 7.7. Unlike the behavior of non-ST U–AMP complexes, U–ADP and U–ATP non-ST complexes (adenine) ring-stack to a *greater* extent than do free nucleotides. The U–ATP complex (non-ST form) dephosphorylates completely to the non-ST U–ADP complex in near-neutral solution within 2 days at 27°, but at higher pD, 9.7, dephosphorylation of U–ATP (ST form) directly to the U–AMP ST complex seems to occur.

The structures and reactions of the complexes in uranyl ion–adenine nucleotide mixtures are of interest because of their possible involvement in uranium inhibition of sugar transport into a biological cell⁴ and because of the use of uranyl compounds in tissue staining.⁵

Potentiometric titration curves of equimolar mixtures (U–ADP and U–ATP) of uranyl nitrate and the adenine 5′-nucleotides, ADP and ATP, depend on the time interval between each addition of base and the subsequent pH measurement.⁶ If pH readings are taken 2 min

after each addition of base, the titration curves show two inflection points (at $r \approx 1.5$, pH ~ 4.5 , and $r \approx 4$, pH ≈ 10 for U–ADP; at $r = 1.0$, pH ~ 4.5 and $r \approx 4.2$, pH ≈ 9.5 for U–ATP,⁷ but three inflection points are seen if pH readings are taken 24 hr after each addition of base. The new inflection is at $r = 3.0$, pH ≈ 7 for both systems. This effect of time is due to acid-producing dephosphorylation which, being most extensive in the $r = 2$ –3 region, causes an inflection point to appear at $r = 3$ within 24 hr.

Structures of the complexes up to the first inflection point deduced from the titrations were treated earlier.⁶ Nmr studies of the U–AMP system in neutral and basic solution were also discussed previously.^{8,9} The present paper describes an nmr investigation of the U–ADP and U–ATP chelate structures in neutral and basic mixtures.

Experimental Section

The experimental procedures and conditions have been described earlier.^{8,9} We wish to emphasize, however, that solubility con-

(1) (a) This paper is based on work performed under contract with the U. S. Atomic Energy Commission at the University of Rochester Atomic Energy Project, and has been assigned Report No. UR-49-1235. It was partially supported by a Special Research Resource Grant, No. RR-00220-07, from the Division of Research Resources of the National Institutes of Health, and by the U. S. Public Health Service Training Grant No. 1T1 DE175. (b) Part of this paper was presented at the Second Rochester Conference on Toxicity at Rochester, N. Y., June 1969.

(2) On leave from University of Roorkee, Roorkee, India.

(3) To whom correspondence and reprint requests should be directed.

(4) L. Hurwitz, Ph.D. Thesis, University of Rochester, Rochester, N. Y., 1953.

(5) M. Beer, *Lab. Invest.*, **14**, 1020 (1965).

(6) I. Feldman, J. Jones, and R. Cross, *J. Amer. Chem. Soc.*, **89**, 49 (1967).

(7) $r =$ moles of $(CH_3)_3NOH$ added/total moles of nucleotide.

(8) R. P. Agarwal and I. Feldman, *J. Amer. Chem. Soc.*, **90**, 6635 (1968); **91**, 2411 (1969).

(9) I. Feldman and K. E. Rich, *ibid.*, **92**, 4559 (1970).